Water Research 289 (2026) 124795

Contents lists available at ScienceDirect

Water Research

journal homepage: www.elsevier.com/locate/watres

# PFAS in stormwater control measures: Removal, distribution, and long-term fate

César Gómez-Ávila [a], Tariq Hussain [b], Balaji Rao [b], Robert Pitt [c], Jennifer Guelfo [b], Huayun Zhou [b], Danny Reible [a,b,*]

[a] Texas Tech University, Department of Chemical Engineering, Lubbock, TX, USA
[b] Texas Tech University, Department of Civil, Environmental, and Construction Engineering, Lubbock, TX, USA
[c] University of Alabama, Department of Civil, Construction, and Environmental Engineering, Tuscaloosa, AL, USA

## HIGHLIGHTS

- Dissolved PFAS are not removed by conventional stormwater treatment.
- Particulate bound PFAS are more likely to be better controlled.
- Sediment resuspension can cause release of particulate-bound PFAS.
- Long residence time systems promote precursor transformation.

## GRAPHICAL ABSTRACT

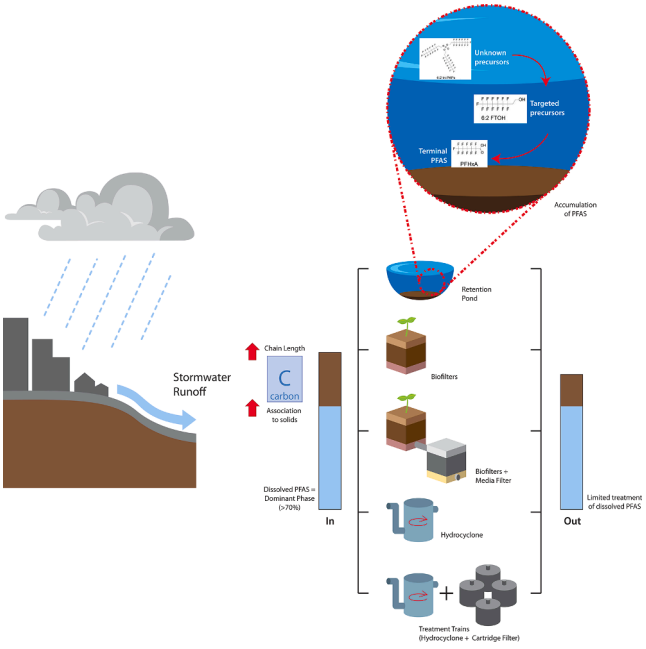


## ARTICLE INFO

*Keywords:*
Stormwater
PFAS
Stormwater control measures

## ABSTRACT

This study evaluates the performance of various conventional stormwater control measures (SCMs) in mitigating 26 per- and polyfluoroalkyl substances (PFAS), including perfluorooctanesulfonic acid (PFOS), and perfluorooctanoic acid (PFOA). PFAS with carbon chain lengths ≥ 9 exhibited greater particulate affinity, ranging

* Corresponding author.
*E-mail address:* danny.reible@ttu.edu (D. Reible).

https://doi.org/10.1016/j.watres.2025.124795
Received 24 May 2025; Received in revised form 16 September 2025; Accepted 11 October 2025
Available online 12 October 2025

Particulates
Dissolved

from 35% to 73% of their concentration associated with suspended solids. In contrast, only 17–35% of PFAS with $C \leq 8$, which dominated the detected compounds, were associated with particulate phases. As most SCMs studied (biofilters, media filters, hydrocyclones, and a retention pond) heavily rely on particle removal, the treatment of filtered-water PFAS (< 0.7 μm) was poor, with essentially no attenuation. Particulate-phase PFAS removal varied, with some systems, such as the retention pond, effectively reducing concentrations. In contrast, others, including the biofilters and one treatment train (hydrocyclone plus cartridge filters), exhibited unexpected increases, suggesting potential remobilization of particulate-associated PFAS within the system. The retention pond SCM, influenced by evaporation, infiltration, and used for local irrigation, was monitored over a one-year period to assess PFAS persistence, precursor transformation, and the effects of water loss on contaminant concentrations. Analysis of precursor compounds in the pond, including fluorotelomer sulfonates (FTS) and perfluoroalkyl sulfonamides (FASAs), showed decreased concentrations relative to runoff. When coupled with increased concentrations of stable products such as perfluorohexanesulfonic acid (PFHxS), PFOS, and PFOA, these changes suggested in situ transformation due to the extended retention time in the system. Additionally, the concentration of PFAS associated with the filtered water (e.g., PFBA, PFOA) increased over time due to evaporation of water during periods of minimal stormwater inputs or discharges. Perfluoroalkane sulfonic acid (PFSA) concentrations (primarily PFOS) in sediments were higher than those in the incoming particulate phase, suggesting sorption and accumulation of PFOS in sediments. The substantial filtered water fraction of PFAS and the limited removal of PFAS by any of the SCMs underscore the limitations of conventional SCMs in treating PFAS.

## 1. Introduction

Per- and polyfluoroalkyl substances (PFAS) are persistent environmental contaminants widely distributed in the environment due to their many industrial and commercial applications (Ahrens and Bundschuh, 2014; Buck et al., 2011; Prevedouros et al., 2006; Schaefer et al., 2023; Zareitalabad et al., 2013). Their high chemical and thermal stability, low volatility, and surfactant behavior have made them useful for fire suppression through aqueous film-forming foams (AFFF), textiles, nonstick coatings, and industrial surfactants (Buck et al., 2011; Kissa, 2001). However, these same properties also contribute to their environmental persistence, raising concerns over their bioaccumulation, mobility, and long-term ecological impacts (Lu et al., 2024; Suja et al., 2009).

AFFF and other industrial discharges have contributed significantly to PFAS contamination in soil, groundwater, surface water, and sediment (Ahmed et al., 2020; Bach et al., 2017; Dauchy et al., 2017; Domingo and Nadal, 2019). Once released into the environment, PFAS partition into various matrices, with perfluoroalkyl carboxylic acids (PFCAs) and perfluoroalkane sulfonic acids (PFSAs) forming as terminal transformation products of precursors such as fluorotelomer sulfonates (FTS) and perfluoroalkyl sulfonamides (FASAs) (LaFond et al., 2023, 2024). Among these, perfluorooctanoic acid (PFOA) and perfluorooctanesulfonic acid (PFOS) are of particular concern due to their widespread occurrence and toxicity (Li et al., 2017; Shi et al., 2024; Tsuda, 2016). Stormwater has been increasingly recognized as a significant nonpoint source of PFAS, mobilizing them from industrial sites, airports, urban surfaces, and other sources into receiving water bodies and sediments (Flanagan et al., 2021; Olmsted et al., 2021). Therefore, effective treatment of stormwater is crucial to prevent the release of PFAS into the environment.

Stormwater Control Measures (SCMs), including biofilters, cartridge filters, hydrocyclones, and retention ponds, are widely implemented to mitigate pollutant loads and manage urban runoff. These systems rely on processes such as filtration, sedimentation, and adsorption; however, their efficiency in reducing contaminant concentrations may vary depending on pollutant characteristics, storm conditions, design, and media composition (Blecken et al., 2017; Gogate et al., 2017; Gomez-Avila et al., 2025; Jay et al., 2019). The effectiveness of these SCMs in removing PFAS remains largely unexplored, especially in evaluating the differences between the treatment of the particulate and filtered-water phases of stormwater runoff. Existing data is often derived from laboratory-scale studies that do not fully capture the complexities of field conditions, including competing constituents, long-term accumulation, and physical fouling of sorption media. Column studies have demonstrated that engineered media amended with biochar or activated carbon can reduce PFAS concentrations (Beryani et al., 2025; Hawkins et al., 2024; Holly et al., 2024; Pritchard et al., 2022), but real-world systems often underperform due to large particle size, low amendment content, and competing agents in stormwater (Beryani et al., 2025). Field-scale studies of biofilters have revealed substantial PFAS accumulation throughout the entire depth of the media, indicating PFAS mobility and the potential for remobilization of previously retained precursors after transformation into more mobile products over time (Beryani et al., 2024). Wetlands have been shown to accumulate PFAS in sediment but may also contribute to recontamination due to shifts in hydrology or sediment chemistry. Precursor transformation further complicates mass balance assessments and our understanding of PFAS fate in these systems (Sarti et al., 2025).

Despite increasing research, several critical gaps remain. Several commonly implemented SCMs, such as media filters and hydrocyclones, have not been evaluated for their effectiveness in PFAS removal. Additionally, comparative field evaluations across different SCMs are limited, particularly regarding the relative behavior of PFAS in filtered water versus particulate phases. There is also limited understanding of long-term system performance, including the effects of evaporation, infiltration, and in situ transformation of precursor compounds. These gaps hinder the ability to design systems that consistently manage both legacy and emerging PFAS under real-world conditions. Retention ponds, a commonly implemented SCM, promote sedimentation, pollutant retention, and controlled stormwater release (Gomez-Avila et al., 2025; Scholz, 2015; Scholz and Yang, 2010), but their role in PFAS fate remains unclear. Due to the persistence and mobility of PFAS, there is concern that retention ponds may function as both sinks and secondary sources of contamination, allowing for potential leaching, diffusion, and remobilization of PFAS over time.

This study characterized the distribution and fate of PFAS in stormwater by sampling surface water, sediment, and stormwater runoff across seven stormwater control measures (SCMs), three biofilters (one with a media filter), three hydraulic separators (two with media filters), and a retention pond. PFAS partitioning between filtered water (< 0.7 μm) and particulate (> 0.7 μm) phases was assessed in all systems. Inlet-outlet comparisons in three storm events (21 total events) were used to evaluate PFAS behavior in these systems, and the retention pond was further examined through additional sampling to assess precursor transformation and PFAS persistence. By focusing on a wide range of SCMs, we hoped to identify trends in PFAS behavior, particularly as it relates to particulate-associated PFAS versus PFAS in filtered water. The results should be viewed as preliminary in that they represent the findings from only these SCMs and the storm events sampled. These findings offer, however, important insights into PFAS behavior in the common mix of SCMs used to address urban and industrial runoff and

inform strategies for more effective stormwater management.

## 2. Materials and methods

### 2.1. SCM and runoff area characteristics

Sites selected for this study were chosen based on their use of operational SCMs designed to mitigate pollutant loads in runoff and follow those previously characterized in a prior study (Gomez-Avila et al., 2025). The selected SCMs encompass a range of treatment strategies, including sedimentation-based systems, filtration media, and combination approaches (treatment trains), to evaluate their effectiveness in PFAS removal. Sampling was conducted across multiple storm events to capture temporal variations in flow conditions and contaminant loading. Understanding the characteristics of runoff areas and land cover is essential for evaluating the performance of SCMs. Runoff amounts and concentrations are directly influenced by the surrounding environment, drainage area size, and rainfall characteristics. While most SCMs in this study were implemented in locations with no known point sources of PFAS contamination, they still exhibited significant concentrations in stormwater. One particular SCM, the retention pond, was located in a drainage area influenced by legacy AFFF contamination, providing a unique case for evaluating PFAS fate and transport in stormwater infrastructure. A summary of site characteristics, including SCM types and sampling periods, is provided in Table 1.

#### 2.1.1. Retention pond SCM (inland southwest)

The retention pond examined in this study was located in the arid southwestern U.S., where rainfall is infrequent but can be intense, leading to potential flooding. All recorded storm events had rain depths between 10 mm and 20 mm. The pond has a surface area of 1.6 hectares and the largest drainage area among all studied systems, covering 104 hectares of mixed-use land. The area of the pond was essentially constant during the period of this study. Approximately half of the drainage area consists of turf, while the remaining portion is dominated by impervious surfaces, including paved areas, parking lots, streets, roofs, and walkways, which contribute to substantial runoff and contaminant transport into the pond.

Four primary drainage pathways contribute to the retention pond. The largest, an unlined channel on the north side, drains a 43-hectare catchment, approximately 50 % of which is impervious. A second pathway, a V-shaped concrete open channel on the northwest side, drains a 17-hectare area where the impervious fraction exceeds 75 %. The third drainage pathway is an 18-inch diameter piped system located on the west side, which drains 32 hectares with over 85 % impervious cover. This area includes a 14-hectare former aircraft parking apron near a historical AFFF use zone, leading to PFAS contamination in the runoff. The final drainage pathway consists of a diffuse sheet-flow entry from a 12-hectare pervious drainage area adjacent to a green space.

#### 2.1.2. Biofilter SCMs (Pacific southwest)

The studied biofilters were located in the Pacific southwest of the U.S., where annual precipitation is low, and there is a distinct rainy season during the winter months. Approximately half of the monitored storm events had rainfall depths below 10 mm, while remaining storms ranged from 10 mm to 40 mm. These biofilters manage relatively small drainage areas, ranging from 0.15 to 0.34 hectares, primarily consisting of parking lots. Over 95 % of the land cover in these areas is impervious, including asphalt and concrete surfaces, which contributed to high runoff volumes and velocities, increasing pollutant transport into the SCMs.

The standalone biofiltration systems included a central drainage

**Table 1**
Summary of sampling sites and specific storm events sampled.

| Location | SCM Type | SCM features | Drainage Type | Drainage Area (hectares) | Storm Event Dates | Rainfall (mm) |
|---|---|---|---|---|---|---|
| Inland Southwest (Continental climate) | Retention Pond | 16,000 $m^2$ pond | Mixed-use Commercial and aircraft parking apron | 104 | 12/26/19–12/28/19<br>10/8/22–10/10/22<br>11/24/22–11/28/22 | 10.9<br>10.7<br>15.2 |
| Pacific Southwest (Coastal climate) | Biofilter 1 | 37 $m^2$ Biofilter | Parking lot | 0.15 | 2/22/20<br>3/3/21<br>3/10/21 | 7.4<br>13.5<br>8.1 |
| | Biofilter 2 | 340 $m^2$ Biofilter | Parking lot | 0.15 | 12/14/21<br>3/28/22–3/29/22 | 30<br>22.4 |
| | Biofilter + Media Filter | 19 $m^2$ Biofilter<br>Bone char and iron-coated activated alumina media filter | Metal fabrication facility + parking lots | 0.34 | 2/10/20–2/11/20<br>2/22/20–2/23/20<br>12/27/20–12/29/20 | 39.9<br>3.8<br>12.4 |
| Pacific Northwest (Coastal climate) | Hydrodynamic separator + Media Filter 1 | Hydrodynamic separator + 23 Zeolite, Perlite, Granular activated carbon (ZPG) cartridge filters | Industrial | 1.8 | 10/9/20–10/10/20<br>11/3/20<br>2/17/21–2/18/21 | 10.4<br>9.7<br>3 |
| | Hydrodynamic separator + Media Filter 2 | Hydrodynamic separator + 23 ZPG cartridge filters | Industrial/ Loading dock | 1.3 | 11/30/21<br>12/4/21 | 9.1<br>2.5 |
| | Hydrodynamic separator | Hydrodynamic separator | Industrial | 1.4 | 2/27/22–2/28/22<br>5/6/22–5/8/22<br>5/28/22 | 114.3<br>13<br>3 |

vault with an underdrain, backflow preventer, approximately 17 inches of biofiltration soil media (BSM) and mulch media, and underlying gravel and stone layers for drainage. Drought-tolerant, low-maintenance vegetation were planted to support treatment performance and system stability. The hybrid biofilter + media filter SCM included three treatment stages: a gabion pretreatment filter, a modular LID biofilter, and a dual-media polishing filter. The gabion, composed of coarse ballast enclosed in geofabric, intercepted runoff and removed gross solids and debris through settling and filtration. Runoff then entered the biofilter, a proprietary vegetated system designed to filter suspended solids and reduce contaminants using a layered media bed consisting of mulch, a sand/peat BSM, bridging stone, and a modular underdrain. Drought-tolerant native vegetation was included in the BSM to maintain infiltration capacity and promote pollutant retention. The final stage, a dual-media filter, included layers of bone char and iron-coated activated alumina (FS-50) within a concrete vault that further targeted sorption of filtered-phase (<0.7 μm) contaminants.

#### 2.1.3. Treatment train SCMs (Pacific northwest)

The SCMs in the northwestern U.S. were in regions where precipitation is more evenly distributed throughout the year, with frequent light to moderate rainfall events. Only three of the recorded storms in this region exceeded 10 mm in total rainfall depth. These SCMs treat runoff from fully impervious industrial catchments ranging from 1 to 1.3 hectares, resulting in high runoff volumes and contaminant loads. The systems included two treatment trains and one standalone system: all three used Continuous Deflective Separation (CDS) hydrodynamic separators, with the two treatment trains also incorporating downstream cartridge filters containing a proprietary blend of zeolite, perlite, and granular activated carbon (ZPG). The CDS unit removed debris and sediment via swirl concentration and deflective screening, while the downstream cartridge filters adsorbed contaminants. Siphon-activated flow through the cartridges ensured even distribution across the media bed, promoting effective treatment and extending media life. Prior to the study, the second treatment train underwent maintenance that included removal of accumulated solids and servicing of the filter cartridges, while the other systems had no recent maintenance activities recorded.

### 2.2. Stormwater sampling

Stormwater sampling protocols followed methodologies established in previous work (Gomez-Avila et al., 2025; Hussain et al., 2024). Composite samples were collected at both influent and effluent points of each SCM using Teledyne ISCO 3700C automatic samplers. Each composite sample consisted of 20 subsamples of 500 mL, collected over the course of a storm event. For the retention pond, automatic samplers were deployed at three of the four identified inlets following the same protocol. The diffuse sheet flow pathway was not sampled due to the difficulty of obtaining representative samples from its shallow and dispersed flow pattern. Additionally, the pervious drainage area was not expected to contribute significant PFAS loads or significant water volume to the retention pond. As the retention pond lacked a discharge outlet for the duration of the project, manual grab samples (5 L each) were collected pre- and post-storm at the north and south sides of the pond. Samples from each side were combined to account for spatial variability and provide a representative concentration for the pond during pre- and post-storm conditions. These composite samples were representative of concentrations within the pond and thus, concentrations in any potential discharges (e.g. irrigation or infiltration). Field and method blanks were employed to assess potential PFAS contamination introduced during sampling. No PFAS were detected in blank samples above method detection limits (~1 ng/L), confirming that the sampling process did not contribute measurable contamination to the collected samples. Detailed descriptions of the sampling and filtration procedures, including quality control measures, are provided in (Gomez-Avila et al., 2025; Hussain et al., 2024) .

### 2.3. Sediment sampling

The retention pond underwent additional sampling of sediments to compare with incoming stormwater particulates. Sediments were collected from the top 5–10 cm at both the north and south ends of the pond. These locations represent areas of primary inflow and potential settling zones. The samples were homogenized to produce a composite representation of recently deposited materials. This approach was designed to capture the upper sediment layer, where stormwater-borne particulates accumulate, allowing for a comparison between incoming particulate-associated PFAS and those retained and potentially altered within the pond through long-term fate processes.

### 2.4. Sample preparation

#### 2.4.1. Water samples

SCM inlet and outlet water samples were processed to quantify the distribution of PFAS between the filtered-water phase (< 0.7 μm) and particulate phase (> 0.7 μm). The fraction of the PFAS in the particulate phase was defined by difference between filtered and unfiltered samples. Concentrations were typically too low to conduct additional fractionation of the particulate phases (i.e. the fraction associated with sand, silt or clay sized particles).

Filtered samples were prepared in 50 mL disposable polypropylene centrifuge tubes. 5 mL of sample were combined with 2.1 mL of LC-MS grade methanol and a mass-labeled PFAS internal standard mix to achieve a final internal standard concentration of 200 ng/L. The resulting mixture, prepared at a 70:30 water-to-methanol ratio, was vortexed for 1 min to ensure thorough mixing. Samples were then centrifuged at 5000 rpm for 20 min. An aliquot of 1.8 mL of supernatant was carefully transferred to an autosampler vial for analysis.

#### 2.4.2. Sediment samples

Sediment samples were extracted using a methanol-based method as described in previous literature (Guelfo et al., 2018; Shojaei et al., 2021). 500 mg of homogenized dry sediment were transferred to a 50 mL disposable polypropylene centrifuge tube and spiked with mass-labeled PFAS internal standard mix to yield a final concentration of 200 ng/L in the extract. Extraction was performed by adding 7 mL of 1 % ammonium hydroxide in methanol, vortexing for 5 s, and placing the sample in a 50°C sonication bath for 1 hour, followed by mechanical shaking for 2 h. The sample was then centrifuged at 5000 rpm for 20 min, and the supernatant was transferred to a 20 mL scintillation vial. This extraction process was repeated twice to maximize analyte recovery. The collected supernatant was evaporated to near dryness under a stream of ultra-pure nitrogen and reconstituted in 700 μL of 1 % acetic acid in methanol. The reconstituted sample was then transferred to a 2 mL microcentrifuge tube containing 40 mg of ENVI-Carb (Millipore Sigma, USA), vortexed for 30 s, and centrifuged at 15,000 rpm for 30 min. The final supernatant was added to a 2 mL autosampler vial containing ultrapure water and LC-MS grade methanol in a 70:30 ratio for analysis.

### 2.5. Chemical analysis

#### 2.5.1. PFAS

PFAS analysis was performed using high-performance liquid chromatography (HPLC) coupled with a Sciex X500R quadrupole time-of-flight mass spectrometer (LC-QTOF-MS, Framingham, MA, USA) in negative electrospray ionization (ESI−) mode. Aliquots of 500 μL of each sample were injected into a C-18 column at 40°C and eluted using HPLC-grade water with 20 mM ammonium acetate and LC-MS-grade methanol at a flow rate of 600 μL/min on an Exion AC pump (Shimadzu). Data collection was implemented in multiple reaction monitoring high resolution (MRMHR) mode. Data were quantified with calibration standards ranging from 0.5 to 5000 ng/L ($R^2$ > 0.99) via isotope dilution.

Continuous calibration checks were performed every ten samples to verify instrument performance. Calibration and Quality control (QC) samples were evaluated based on the recovery of internal standards, and only those with recoveries between 70 % and 130 % were accepted. Samples outside this range were reanalyzed. Calibration and mass-labeled internal standards were obtained from Wellington Laboratories (Guelph, Ontario, Canada). A total of 26 PFAS were analyzed, including PFCAs (C4–C14), PFSAs (C4–C10), sulfonamides (FBSA, FHxSA, PFOSA), FTS (4:2, 6:2, 8:2), and sulfonamidoacetic acids (N-MeFOSAA, N-EtFOSAA); 16 compounds were consistently detected above method detection limits (1–10 ng/L for most PFAS) and included in the data analysis: PFBA, PFPeA, PFHxA, PFHpA, PFOA, PFNA, PFDA, PFBS, PFPeS, PFHxS, PFOS, FBSA, FHxSA, PFOSA, 6:2 FTS, and 8:2 FTS, while PFAS that were never detected included PFTrDA, PFTeDA, PFNS, PFDS, N-MeFOSAA, and N-EtFOSAA. The sum of the 16 consistently detected compounds is referred to as $\sum_{16}PFAS$ throughout the manuscript. The sum was dominated by five PFAS: PFHxA, PFOA, PFHxS, PFOS and FHxSA, which typically constituted the vast majority of the measured compounds. Further details such as their respective mass-labeled internal standards, molecular weights, and full compound names are further described in Tables S1 and S2 of the supplementary information (SI).

#### 2.5.2. Total oxidizable precursor assay (TOP)

The TOP assay was conducted following the method by (Houtz and Sedlak, 2012), with modifications from (Shojaei et al., 2021). A 5 mL aqueous sample was transferred to an 8 mL glass vial containing 80 mM potassium persulfate and 170 mM sodium hydroxide. The mixture was heated in a water bath at 80°C for 8 h. After cooling to room temperature, the pH was measured to ensure it remained between 5 and 9; if the pH dropped below 3 (which can lead to PFCA mineralization), samples were discarded, and the procedure was repeated. After oxidation, samples were mixed with LC-MS grade methanol in a 70:30 ratio and spiked with mass-labeled internal standards. For sediment samples, 500 mg of dry sediment were extracted without mass-labeled internal standards for the TOP assay, and the final extract (1 % acetic acid in methanol) was reconstituted in 5 mL of ultrapure water after nitrogen evaporation. The remaining TOP assay procedure was performed as described for aqueous samples. Following the TOP assay, samples were analyzed as described above.

#### 2.5.3. Chloride analysis

Chloride concentrations in stormwater samples from all outfalls and in retention pond water (pre- and post-storm) were measured using ion chromatography, following EPA Method 300.1 (USEPA, 1997) and are presented in Table S3. Calibration was performed over the concentration range of 1–200 ng/L, with quality-control standards deemed acceptable only if measured values fell within ±20 % of their nominal concentrations.

### 2.6. Retention pond mass balance

To evaluate seasonal dynamics of PFAS in the retention pond, monthly grab samples and water level measurements were collected between January and December 2022. Water samples were analyzed for PFAS and chloride concentrations, with changes in chloride and water level changes providing a record of volumetric change over time. This data was used to develop a mass balance model simulating hydrologic fluctuations and PFAS behavior throughout the year.

The model was initialized using data from a storm that occurred on November 25–26, 2022 (17 mm of total precipitation). This event served as a baseline for estimating pond volume. A chloride mass balance was applied under the assumptions that short-term losses such as infiltration and evaporation were negligible over the timescale of a single storm, and that the pond acted as a thoroughly mixed tank. Runoff volumes from each outfall were calculated using the United States Department of Agriculture (USDA) curve number approach and precipitation information from the West Texas Mesonet (Mesonet, 2025). By combining chloride concentrations from the pond and the runoff sources, the unknown pre-storm pond volume was calculated (Equation 1, SI). The water balance yielded a pre-storm volume of $4.5 \times 10^4$ m$^3$ (Nov 24) and a post-storm volume of $5.1 \times 10^4$ m$^3$ (Nov 28), giving an average pond depth of 3.1 m

Following this initialization, the model estimated volume changes in daily intervals, incorporating direct rainfall, runoff contributions, and evaporation. The only unknowns were losses via infiltration and irrigation, which were inferred by comparing the modeled water levels to the monthly field measurements. This comparison enabled calibration of the model and estimation of loss terms. Results indicated that infiltration was negligible, consistent with expectations for a pond with a compacted fine silt base that retains water year-round. From January through May, volume losses were attributed solely to evaporation, which was quantified using reference data from the Water Data for Texas database, which provides evaporation rates specific to the region. During warmer months, observed losses increased substantially and were attributed to irrigation withdrawals for nearby landscaping. Estimated losses reached a maximum of approximately 1400 m$^3$/day, equivalent to a depth reduction of roughly 0.1 m/day over the 16,000 m$^2$ pond surface area—values consistent with expected irrigation demands for similar systems. Additional modeling details, including water balance equations, runoff volumes, and verification of modeled pond depths with field observations, are presented in the SI (Figures S1–S3).

After establishing the dynamics of pond volume, the model was extended to estimate PFAS concentrations over time. Stormwater runoff concentrations, averaged across three sampled storm events, were used as PFAS inputs, and direct rainfall to the pond was assumed to contain negligible PFAS. The variation in individual PFAS concentrations from the pond inputs during the three main events were small (± 50 % for PFOA and 36 % for PFOS) and thus were assumed constant during all storm events for the purposes of the model. PFAS removal was modeled conservatively under the assumption that PFAS did not degrade or evaporate and exited the pond only through irrigation or infiltration, carrying the same concentration as the bulk pond water. Modeled and measured concentrations for each detected PFAS are shown in the SI (Figures S4–S16).

## 3. Results and discussion

### 3.1. Stormwater characterization

To characterize stormwater entering the SCMs, the distribution of PFAS between the filtered-water and particulate phases was evaluated to assess how PFAS partitioning varies with carbon chain length and chemical class. Fig. 1 presents the proportion of total PFAS concentration in particulates compared to the filtered water. Total sample size is 153, including biofilters ($n = 41$), retention pond ($n = 61$), and hydrocyclones and media filters ($n = 51$). Results show a trend of increasing PFAS association with particulates as fluorinated carbon chain length increases, suggesting that longer-chain PFAS exhibit greater affinity for solid-phase partitioning than shorter-chain compounds, a pattern that is consistent with previous studies (Guelfo and Higgins, 2013; Higgins and Luthy, 2006). Statistical analysis using ANOVA ($\alpha = 0.05$) identified a significant difference in PFAS distribution across carbon chain length groups and, in particular, the fraction of C5, C6 and C7 PFAS associated with particulates was significantly less than both shorter chain length and longer chain length PFAS ($p = 0.007$). PFAS with $C \geq 9$ had median particulate-phase associations exceeding 35 %, with values reaching over 70 %, presumably due to the dominance of hydrophobic interactions. Although PFAS with $C \leq 8$ were primarily detected in the filtered-water, a notable fraction was still present in particulates, particularly for C3 and C4 PFAS, possibly due to increasing significance of electrostatic interactions. The median particulate association for

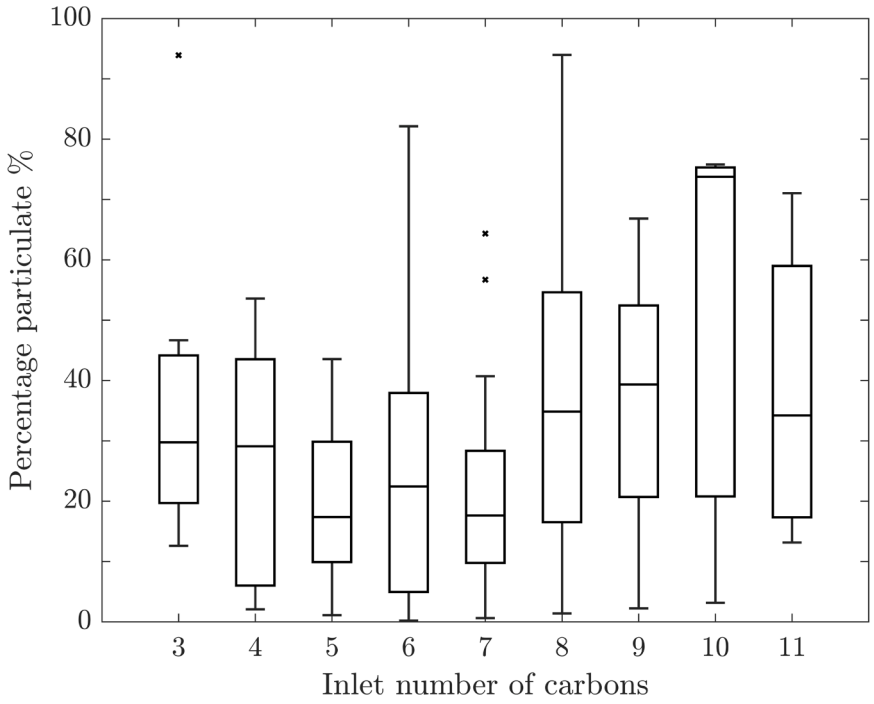


**Fig. 1.** Percentage of total PFAS concentration present in inlet particulates (> 0.7 μm) for all SCMs divided by fluorinated carbon chain length ($n$ = 153).

PFAS with $C \leq 8$ ranged from below 20 % to 30 %, with some variability across stormwater samples. A separate comparison of PFCAs and PFSAs association with particulates did not show a statistically significant difference, indicating that carbon chain length, rather than functional group, plays a primary role in PFAS partitioning behavior in stormwater particulates. Additionally, the variability in solids content across sites can obscure clear trends based solely on chain length, which limits the ability to more clearly isolate the effect of chain length or functional group on the fraction associated with particulates.

### 3.2. SCM PFAS capture efficiency

The effectiveness of SCMs in reducing PFAS concentrations varied across the systems studied. Fig. 2 summarizes the total PFAS concentrations ($\sum_{16}PFAS$, as defined in section 2.5.1) at the inlet and outlet of each SCM, using mean values from all sampled storms as identified in Table 1. Fig. 2(a) shows the filtered-water $\sum_{16}PFAS$, while Fig. 2(b) shows the same quantity in the particulate fraction. Error bars indicate the range (high and low) of the data across all sampled storm events. Note that this figure does not capture inlet-outlet paired data but simply the range of inlet and outlet concentrations across all storm events for each system. Due to the number of sampling events per system, these findings should be viewed as preliminary trends, for which a more in depth sampling is necessary to fully understand PFAS fate within SCMs.

Across most systems, apparent removal of filtered-water (<0.7 μm) PFAS was minimal, with effluent concentrations generally between 10 and 50 ng/L, except in the retention pond, where post-storm pond concentrations reached nearly 1400 ng/L (approximately two orders of magnitude higher). These results are consistent with previous findings (Gomez-Avila et al., 2025), highlighting that the tested SCMs show low removal efficiency for filtered-water contaminants. Among all systems evaluated, only the biofilters and one hydrocyclone plus cartridge filter system demonstrated reductions in filtered-water PFAS. Biofilter 1 reduced concentration from over 100 ng/L to 51 ng/L, and Biofilter 2 reduced concentrations from 71 ng/L to 32 ng/L. A possible explanation for this reduction is the use of mulch and sand/peat-based biofiltration soil media (BSM). The organic content in the mulch and peat BSM can contribute to contaminant retention (Higgins and Luthy, 2006; Milinovic et al., 2015), and the established vegetation may support some degree of PFAS uptake as has been seen in literature (Awad et al., 2022; Higgins and Luthy, 2006; Milinovic et al., 2015). The hydrocyclone plus cartridge filter system, which reduced filtered-water PFAS concentrations from 48 ng/L to 24 ng/L, was the system that underwent maintenance prior to sampling. This maintenance likely allowed for more effective contact between stormwater and the ZPG filter media, enabling sorption of filtered PFAS. In contrast, the second hydrocyclone plus cartridge filter system, which had not been recently maintained, exhibited increased effluent concentrations. The accumulation of solids in the hydrocyclone vault and media cartridges likely led to physical clogging, reduced flow-through, and limited contact between stormwater and the filter media. These conditions can significantly impair the performance of sorptive systems, even when using granular activated carbon, a material well established for PFAS removal (Liu et al., 2019; McCleaf et al., 2017; Simonich et al., 2022), although additional studies are necessary to fully understand this behavior. The remaining systems exhibited little to no filtered removal, either due to influent concentrations near detection limits or to a lack of optimization for PFAS treatment.

Treatment of particulate-associated PFAS (i.e., those retained on 0.7 μm filters), which accounted for 15–40 % of total PFAS, was inconsistent, likely due to their inconsistent removal of the smallest particles. The concentrations of solid-associated PFAS in many of the systems were of the order of 10 ng/L or less, which is near the limit of detection for the $\sum_{16}PFAS$. While PFAS with carbon chain lengths $\geq 9$ are expected to bind with solids (Section 3.1) and be removed via sedimentation or filtration, the majority of PFAS detected in these systems had chain lengths below this threshold. Several systems exhibited elevated particulate-associated PFAS concentrations at the outlet, possibly due to desorption from surfaces or resuspension of sediments within the SCMs that lacked maintenance. For example, the first hydrocyclone + cartridge filter system showed an overall increase in PFAS, primarily driven by the particulate phase. Maintenance and regular removal of accumulated solids, plus designs to minimize scour of previously captured fine particulates, are needed for hydrocyclone systems to achieve good solids removal during stormwater events. The second Hydrocyclone + Cartridge Filter system (which had undergone maintenance) achieved

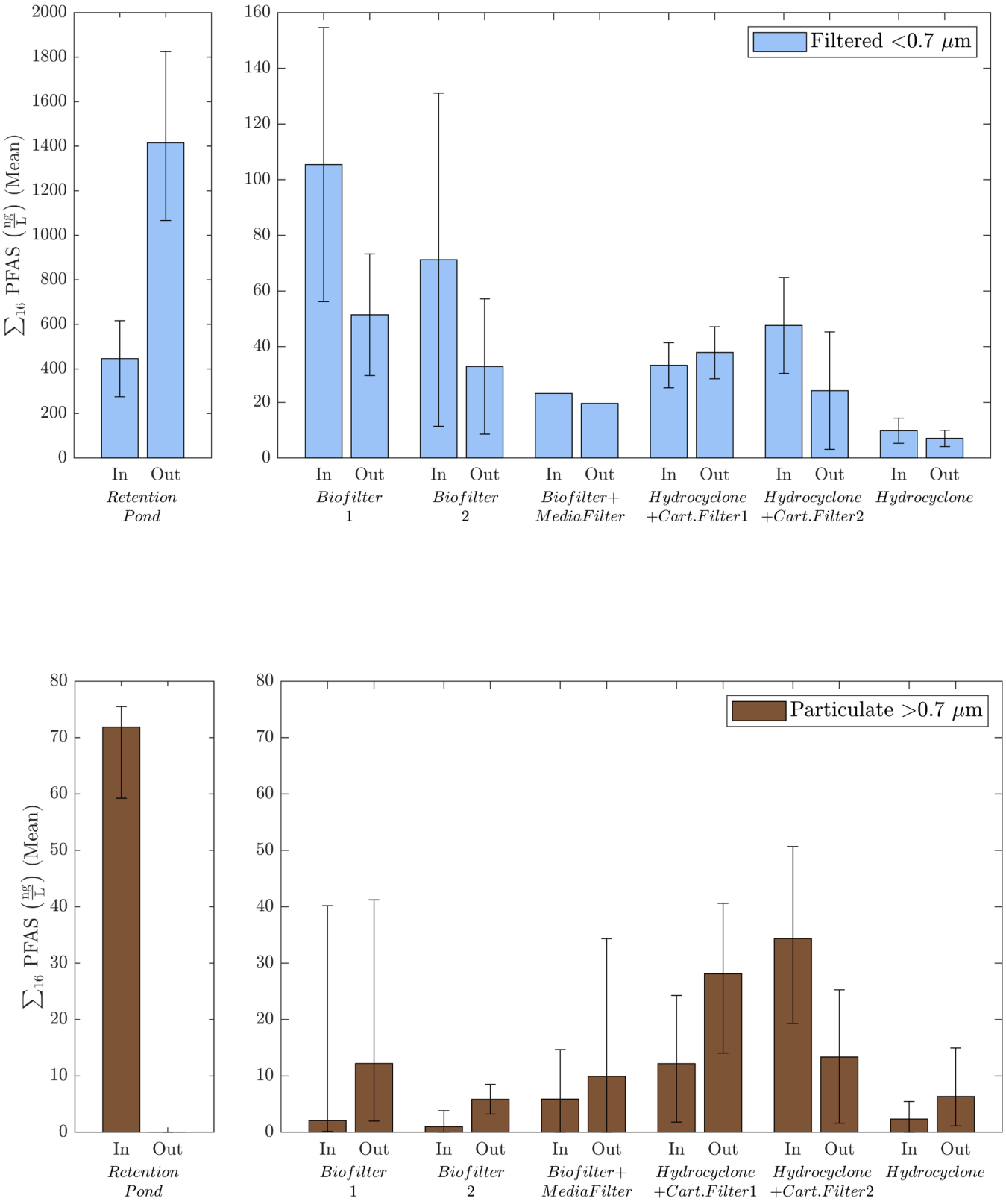


**Fig. 2.** (a) Mean inlet and outlet filtered water (< 0.7 μm) concentrations (ng/L) and range of measuremetns over all events of $\sum_{16}$PFAS for each SCM. (b) Mean inlet and outlet particulate (> 0.7 μm) concentrations (ng/L) and range over all events of $\sum_{16}$PFAS for each SCM.

notable reductions in particulate-phase PFAS, decreasing from 34 ng/L to 13 ng/L (a 61 % reduction), supporting the idea that solids removal is possible, but highlighting the need for additional studies.

The retention pond exhibited different behavior from other SCMs due to the presence of a known PFAS source and its ability to capture very small particulates. While it effectively removed particulate-phase PFAS via sedimentation and mixing within the large pond volume, it showed a significant increase in filtered-phase PFAS, from

approximately 450 ng/L at the inlet to a maximum of 1400 ng/L in the pond (and presumably in any pond discharges). This accumulation likely reflects the lack of a consistent discharge, the persistence of PFAS in the water column due to their stability and their low volatility, combined with evaporation of water in the pond. These dynamics are explored further in Section 3.3.

Fig. 3 presents the mean relative abundance of PFAS in the inlet and outlet by phase for all systems except for the retention pond. As noted above, the retention pond exhibited significant differences as a result of a specific known source (AFFF associated with airfield operations). PFAS in all other systems were not linked to a particular source and likely represent a more diffuse background of PFAS from multiple sources. The PFAS in Fig. 3, are color-coded by class: red for perfluoroalkyl sulfonates (PFSAs), blue for perfluoroalkyl carboxylates (PFCAs), and yellow for precursors such as fluorotelomer sulfonic acids (FTSs) and perfluoroalkane sulfonamides (FASAs). Within each class, darker tones indicate longer-chain compounds.

When comparing inlet and outlet distributions, the filtered-water PFAS composition showed minimal overall changes, highlighting the limited effectiveness of SCMs in the removal of PFAS in the <0.7 μm fraction. However, some compound-specific shifts were observed. Precursors such as FASAs were completely removed from the filtered phase, and slight reductions in FTS were detected, suggesting potential sorption and filtration. These changes were accompanied by an increase in FTS within the particulate fraction at the outlet, supporting the possibility of sorption from the dissolved to the particulate phase. Within the inlet itself, PFCAs were more abundant in the filtered-water, with 45 % of total PFAS (21 % PFOA) but less dominant in the particulate fraction with only 29 % of total PFAS (10 % PFOA). PFSAs were relatively consistent across phases, accounting for 30 % of filtered-water PFAS (27 % PFOS) and 27 % of the particulate (17 % PFOS). Precursors were notably more abundant in the particulate phase, with a total of 44 % of total PFAS compared to 25 % in the filtered water. At the outlet, PFSAs showed a notable increase, mostly in the particulate fraction, rising to 58 % compared to 38 % in the filtered water. This shift may be due to transformation of precursor compounds initially sorbed to retained sediments in the systems.

### 3.3. Retention pond PFAS distribution and dynamics

To investigate the mechanisms behind PFAS accumulation in the retention pond, the distribution of different PFAS classes between surface water and sediment was evaluated and their relative composition is shown in Fig. 4.

Precursors (FTS and FASAs) account for 27–29 % of the total concentration in incoming stormwater (both filtered and particulate) but decrease to < 10 % of the concentrations in the pond and underlying sediment. This suggests that transformation processes within the pond contribute to the degradation of precursors into terminal PFAS, supported by an observed increase in terminal compound distribution such

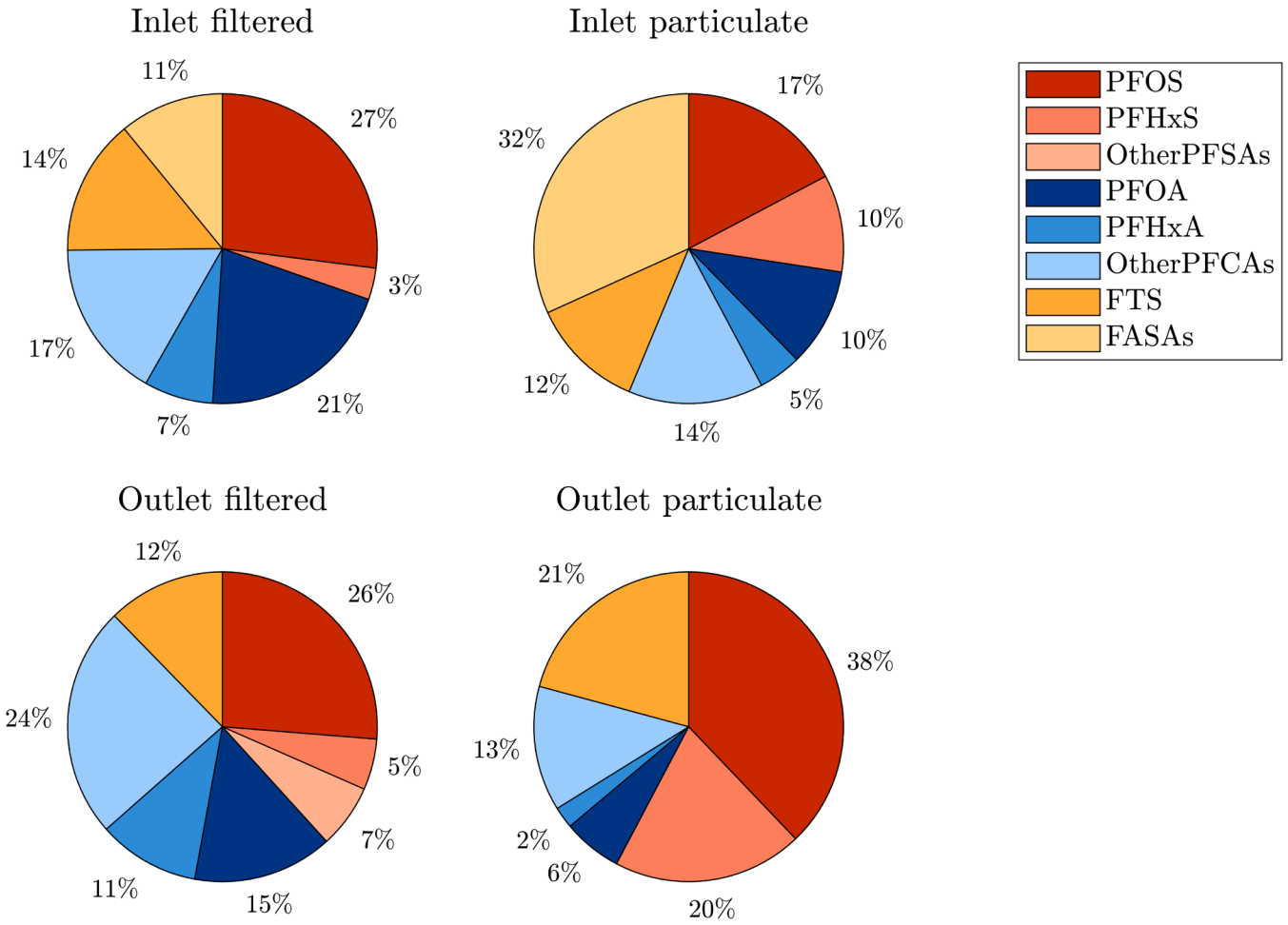


**Fig. 3.** Relative abundance of PFAS in the SCMs over the 18 storm events (excluding the retention pond). The top row represents inlet samples, with filtered-water PFAS (< 0.7 μm) on the left ($n = 181$) and particulate-associated PFAS (> 0.7 μm) on the right ($n = 180$). The bottom row shows outlet samples with filtered-water PFAS (< 0.7 μm) on the left ($n = 267$) and particulate-associated PFAS (> 0.7 μm) on the right ($n = 267$). PFAS are color coded by class: PFSAs (red), PFCAs (blue), and precursors (yellow), with increasing color saturation indicating longer carbon chain lengths.

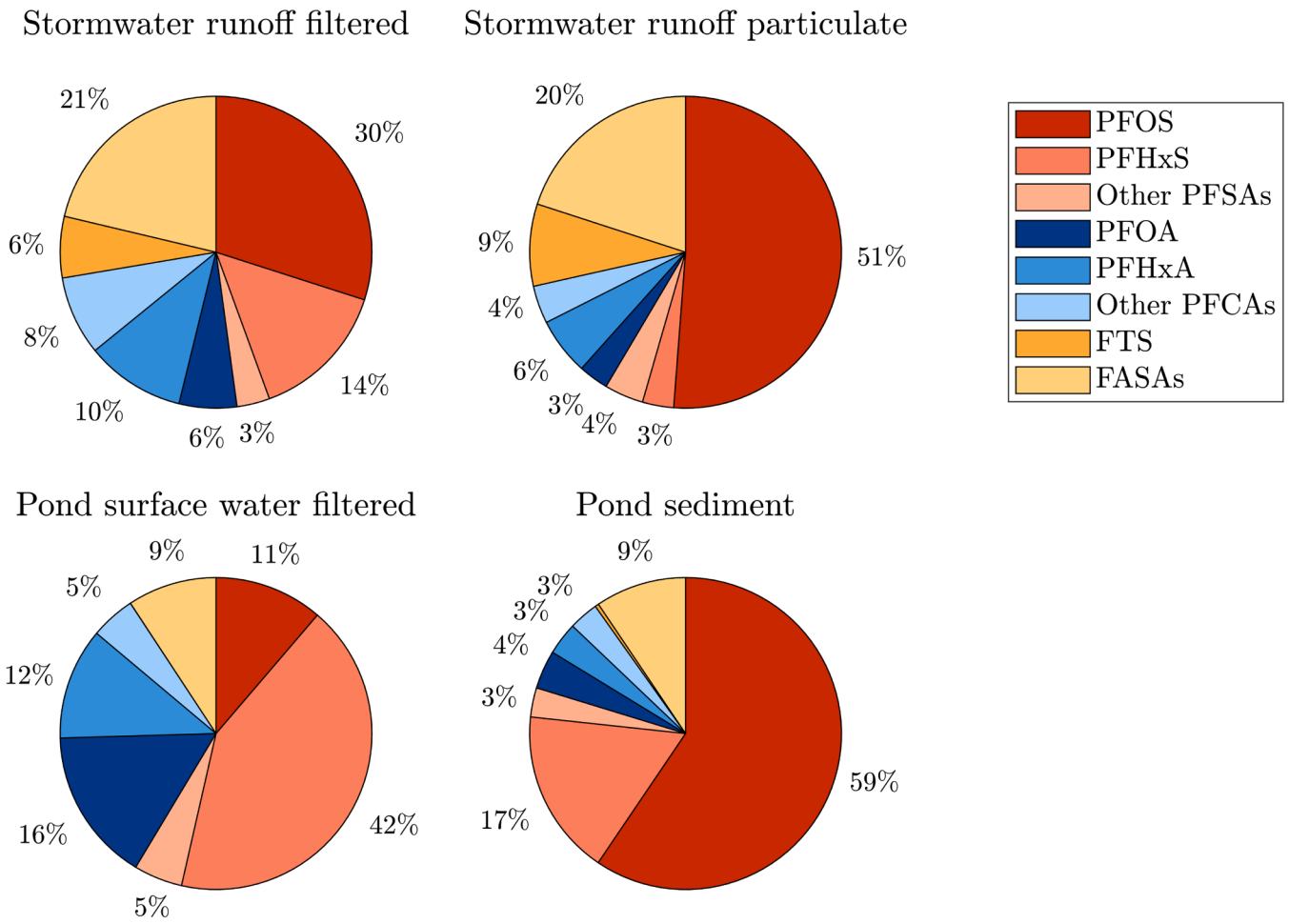


**Fig. 4.** Relative abundance of PFAS in the retention pond. The top row represents stormwater runoff samples during three storm events, with filtered-water PFAS (< 0.7 μm) on the left ($n = 128$) and particulate-associated PFAS (> 0.7 μm) on the right ($n = 128$). The bottom row shows retention pond samples during the events and sampling over a year with filtered-water PFAS (< 0.7 μm) on the left ($n = 322$) and particulate-associated PFAS (> 0.7 μm) on the right ($n = 113$). PFAS are color coded by class: PFSAs (red), PFCAs (blue), and precursors (yellow), with increasing color saturation indicating longer carbon chain lengths.

as PFHxS and PFOA in pond water. In the pond surface water, PFCAs account for over 30 % of the total PFAS concentration, but drop below 10 % in sediment, consistent with the relatively low organic carbon–-water partitioning coefficients of short to medium-chain acids such as PFHxA (log $K_{oc}$ of 1.99 – 2.26), which remain more mobile in the water column. Conversely, longer chain PFSAs which have higher log $K_{oc}$ values (e.g., PFOS 3.8 – 4.8) constitute 58 % of the filtered-water PFAS and increase to 80 % in sediment. A similar trend is seen when comparing PFAS in incoming particulates and pond sediment. While both exhibit comparable distributions, sediment contains a lower proportion of precursors, further supporting in-situ transformation over time. Additionally, although PFOS constitutes about 30 % of total PFAS in incoming stormwater, its portion drops to 11 % in pond water. In contrast, PFOS increases in sediment, rising from 51 % in stormwater particulates to 59 % in pond sediment, possibly through a combination of repartitioning from the water column into the sediment and precursor transformation. Results of the TOP assay (Fig. 5) demonstrate that precursor oxidation can significantly increase (more than double) the molar concentration of PFAS in the system. The greater increase in PFCAs, relative to the total measured precursors suggests the presence of additional, unidentified precursors not captured by targeted analysis. Additionally, targeted precursors may represent transitional compounds in the transformation pathway from unknown precursors to terminal PFAS (LaFond et al., 2023). In the natural environment of the pond, photolysis and microbial activity are likely responsible for driving transformation of these precursors into terminal PFAS (Houtz and Sedlak, 2012).

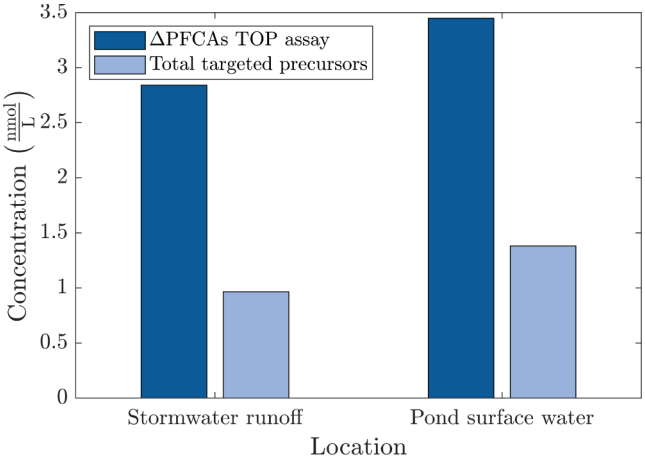


**Fig. 5.** Comparison of molar concentrations (nmol/L) between the increase in PFCAs from the TOP assay and the total targeted precursors in stormwater runoff and pond surface water.

Monthly measurements and modeling (Section 2.6) of water level and $\sum_{16}PFAS$ concentrations provide some further insight into pond dynamics as shown in Fig. 6. The model of pond water volume included

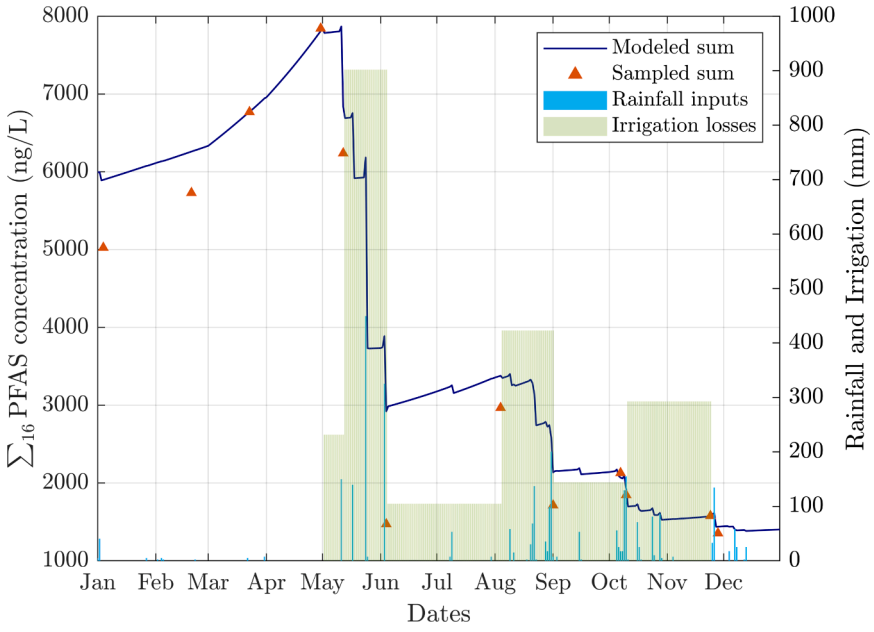


**Fig. 6.** Modeled and measured $\Sigma_{16}$ PFAS concentrations within the retention pond, including daily associated rainfall inputs and irrigation losses.

estimated storm inputs, evaporation losses, and estimated discharges (primarily irrigation) by differences with measured volume. The model of PFAS concentrations included inputs due to storm events (estimated from the sampled storms), increases in concentration due to evaporation, and loss of water and PFAS mass (but no change in concentration) due to irrigation discharges. Differences between measured and predicted PFAS concentrations are likely due to the settling of particulate-associated PFAS and transformation of precursors, neither of which are quantified in the model.

Prior to the modeling period, high-PFAS groundwater was occasionally used to fill the pond to ensure adequate irrigation volume, which led to a relatively high PFAS concentration at the start of the sampling period, as shown in Fig. 6. This input was permanently eliminated in March 2022, and pond volume observations also suggest that there was no additional groundwater input between January and March. From January through May, pond volume declined primarily via evaporation with no significant rain inputs or irrigation discharges. Significant rainfall in May and June increased pond volume and diluted PFAS across all classes. Between storm events, periodic irrigation withdrawals removed both water and associated PFAS mass. These losses were estimated by comparing modeled PFAS inputs with observed volume changes, assuming negligible infiltration due to the pond's fine-silt base and the observed water surface elevation changes accounted for by evaporation. For the remainder of the year, stormwater inputs and withdrawals reached an approximate balance, resulting in only modest PFAS fluctuations and suggesting a dynamic equilibrium among dilution, concentration, transformation, and mass export processes.

Further understanding of relevant processes can be gained from examination of individual PFAS. During the January to May period, the shorter-chain filtered-water PFAS (PFBA, PFHxA, PFHxS) increased by nearly 50 %, aided in part by precursor degradation. At the same time, PFOS (log $K_{oc} \approx 2.6$–$3.8$) concentrations decreased by approximately 20 %, reflecting its strong affinity for solids and retention in the pond due to solids settling. Plots of modeled and observed concentrations of these compounds can be found in SI. These findings underscore the critical need to incorporate both transformation pathways and sediment interactions into PFAS fate models for retention ponds.

The absence of effective natural removal mechanisms leads to the accumulation of terminal PFAS in sediments and the water column. Pond volume and evaporation govern overall PFAS concentrations, and without active treatment targeting PFAS compounds, stormwater control systems that rely on standing water will exhibit progressive PFAS buildup and increasing concentrations over time.

## 4. Conclusions

By evaluating PFAS distribution across different phases and stormwater control measures (SCMs), this study identifies key processes that influence PFAS fate and retention. The main findings are:

- PFAS partitioning to solids is positively correlated with carbon chain length, with long-chain PFAS showing stronger partitioning to particulates. For PFAS with more than eight fluorinated carbons ($C > 8$), the median concentration found in the particulate phase is at least 35 %, increasing with chain length, reinforcing the role of particle interactions in PFAS transport and treatment.
- The evaluated SCMs were ineffective at removing filtered-water ($<$ 0.7 μm) PFAS, as most conventional treatments heavily rely on particle removal for treatment. Additionally, filtered-water PFAS dominated total concentrations across most sites.
- SCMs are designed to effectively remove particulate associated contaminants, but the observed results were inconsistent. The variability reflected low solids and PFAS concentrations on particles (often near detection limits), as well as occasional increases in effluent solids due to accumulation and resuspension of solids during storm events for some systems. Regular removal of the accumulated solids should reduce or eliminate these issues.
- PFAS speciation in the SCMs revealed that perfluoroalkyl sulfonates (PFSAs) were predominantly found in sediments, while perfluoroalkyl carboxylates (PFCAs) remained more prevalent in the filtered water. The observed depletion of precursor compounds relative to incoming stormwater, along with elevated concentrations of degradation products, suggests in situ transformation into terminal PFAS in systems with long residence times.
- Long-residence time systems (such as closed retention ponds) can also lead to accumulation of PFAS over time and increases in water concentrations over time due to the low volatility of most PFAS and water loss processes such as evaporation.
- Long-residence time systems can also lead to accumulation of PFAS in sediments for relatively strongly sorbing PFAS such as PFOS. The

inherent stability of terminal PFAS allows them to persist unless physically removed or treated.
- As a result of both of the previous points, long-residence time systems can result in both sediments and standing water acting as long-term PFAS sinks which must be prioritized in monitoring and remediation strategies.
- PFAS were detected at levels exceeding regulatory thresholds even at sites without known AFFF contamination, suggesting that stormwater can be a substantial source of PFAS for potential drinking water sources. Regular maintenance, monitoring, and potential infrastructure upgrades will be necessary to mitigate these hidden sources.

The results represent trends observed for the specific SCMs and storm events sampled, and more comprehensive sampling would be required to assess detailed performance and mechanisms for any specific SCM. The general trends observed suggest that traditional SCMs are expected to offer partial mitigation for particulate-phase PFAS but have limited impact on filtered-water contaminants, underscoring the urgent need for targeted treatment technologies for PFAS. As industrial practices move toward greater use of hexafluoropropylene oxide dimer acid (HFPO-DA), also known as GenX, the proportion of PFAS in the filtered phase is expected to increase, further reducing the effectiveness of conventional SCMs. This work highlights the need for SCM designs that incorporate targeted removal mechanisms for filtered-water PFAS and consideration of long-term PFAS behavior when developing stormwater management strategies that prevent their long-term accumulation within stormwater systems.

## CRediT authorship contribution statement

**César Gómez-Ávila:** Writing – original draft, Visualization, Investigation, Formal analysis, Conceptualization. **Tariq Hussain:** Formal analysis, Data curation. **Balaji Rao:** Writing – review & editing, Supervision, Conceptualization. **Robert Pitt:** Writing – review & editing, Methodology. **Jennifer Guelfo:** Writing – review & editing, Methodology. **Huayun Zhou:** Formal analysis. **Danny Reible:** Writing – review & editing, Supervision, Project administration, Conceptualization.

## Declaration of competing interest

The authors declare the following financial interests/personal relationships which may be considered as potential competing interests: Danny Reible reports financial support was provided by Strategic Environmental Research and Development Program. Danny Reible reports financial support was provided by JF Maddox Foundation. If there are other authors, they declare that they have no known competing financial interests or personal relationships that could have appeared to influence the work reported in this paper.

## Acknowledgments

This work was supported by SERDP grant ER18–1371; and the JF Maddox Foundation.

## Supplementary materials

Supplementary material associated with this article can be found, in the online version, at doi:10.1016/j.watres.2025.124795.

## Data availability

Data will be made available on request.

## References

Ahmed, M., Johir, M., McLaughlan, R., Nguyen, L.N., Xu, B., Nghiem, L.D., 2020. Per-and polyfluoroalkyl substances in soil and sediments: occurrence, fate, remediation and future outlook. Sci. Total Environ. 748, 141251.
Ahrens, L., Bundschuh, M., 2014. Fate and effects of poly-and perfluoroalkyl substances in the aquatic environment: a review. Environ. Toxicol. Chem. 33 (9), 1921–1929.
Awad, J., Brunetti, G., Juhasz, A., Williams, M., Navarro, D., Drigo, B., Bougoure, J., Vanderzalm, J., Beecham, S., 2022. Application of native plants in constructed floating wetlands as a passive remediation approach for PFAS-impacted surface water. J. Hazard. Mater. 429, 128326.
Bach, C., Dauchy, X., Boiteux, V., Colin, A., Hemard, J., Sagres, V., Rosin, C., Munoz, J.-F., 2017. The impact of two fluoropolymer manufacturing facilities on downstream contamination of a river and drinking water resources with per-and polyfluoroalkyl substances. Environ. Sci. Pollut. Res. 24, 4916–4925.
Beryani, A., Flanagan, K., You, S., Forsberg, F., Viklander, M., Blecken, G.-T., 2025. Critical field evaluations of biochar-amended stormwater biofilters for PFAS and other organic micropollutant removals. Water Res. 281, 123547.
Beryani, A., Furén, R., Osterlund, H., Tirpak, A., Smith, J., Dorsey, J., Winston, R.J., Viklander, M., Blecken, G.-T., 2024. Occurrence, concentration, and distribution of 35 PFASs and their precursors retained in 20 stormwater biofilters. Environ. Sci. Technol. 58 (32), 14518–14529.
Blecken, G.-T., Hunt III, W.F., Al-Rubaei, A.M., Viklander, M., Lord, W.G, 2017. Stormwater control measure (SCM) maintenance considerations to ensure designed functionality. Urban Water J. 14 (3), 278–290.
Buck, R.C., Franklin, J., Berger, U., Conder, J.M., Cousins, I.T., De Voogt, P., Jensen, A. A., Kannan, K., Mabury, S.A., van Leeuwen, S.P., 2011. Perfluoroalkyl and polyfluoroalkyl substances in the environment: terminology, classification, and origins. Integr. Environ. Assess. Manag. 7 (4), 513–541.
Dauchy, X., Boiteux, V., Bach, C., Rosin, C., Munoz, J.-F., 2017. Per-and polyfluoroalkyl substances in firefighting foam concentrates and water samples collected near sites impacted by the use of these foams. Chemosphere 183, 53–61.
Domingo, J.L., Nadal, M., 2019. Human exposure to per-and polyfluoroalkyl substances (PFAS) through drinking water: a review of the recent scientific literature. Environ. Res. 177, 108648.
Flanagan, K., Blecken, G.-T., Osterlund, H., Nordqvist, K., Viklander, M., 2021. Contamination of urban stormwater pond sediments: a study of 259 legacy and contemporary organic substances. Environ. Sci. Technol. 55 (5), 3009–3020.
Gogate, N.G., Kalbar, P.P., Raval, P.M., 2017. Assessment of stormwater management options in urban contexts using multiple attribute decision-making. J. Clean. Prod. 142, 2046–2059.
Gomez-Avila, C., Rao, B., Hussain, T., Zhou, H., Pitt, R., Colvin, M., Hayman, N., DeMyers, M., Reible, D., 2025. Particle size-based evaluation of stormwater control measures in reducing solids, polycyclic aromatic hydrocarbons (PAHs) and polychlorinated biphenyls (PCBs). Water Res., 123299
Guelfo, J.L., Higgins, C.P., 2013. Subsurface transport potential of perfluoroalkyl acids at aqueous film-forming foam (AFFF)-impacted sites. Environ. Sci. Technol. 47 (9), 4164–4171.
Guelfo, J.L., Marlow, T., Klein, D.M., Savitz, D.A., Frickel, S., Crimi, M., Suuberg, E.M., 2018. Evaluation and management strategies for per-and polyfluoroalkyl substances (PFASs) in drinking water aquifers: perspectives from impacted US Northeast communities. Environ. Health Perspect. 126 (6), 065001.
Hawkins, K.M., Pritchard, J.C., Struck, S., Cho, Y.-M., Luthy, R.G., Higgins, C.P., 2024. Controlling saturation to improve per-and polyfluoroalkyl substance (PFAS) removal in biochar-amended stormwater bioretention systems. Environ. Sci. 10 (5), 1233–1244.
Higgins, C.P., Luthy, R.G., 2006. Sorption of perfluorinated surfactants on sediments. Environ. Sci. Technol. 40 (23), 7251–7256.
Holly, M.A., Gunn, K.M., Keymer, D., Sanford, J.R., 2024. Evaluation of per-and polyfluoroalkyl substances leaching from biosolids and mitigation potential of biochar through undisturbed soil columns. ACS ES&T Water 4 (2), 413–426.
Houtz, E.F., Sedlak, D.L., 2012. Oxidative conversion as a means of detecting precursors to perfluoroalkyl acids in urban runoff. Environ. Sci. Technol. 46 (17), 9342–9349.
Hussain, T., Athanasiou, D., Rao, B., Bejar, M., Rakowska, M., Drygiannaki, I., Chadwick, D.B., Colvin, M.A., Hayman, N.T., Rosen, G.H., 2024. Sediment recontamination potential and biological impacts of hydrophobic organics from stormwater in a mixed-use watershed. Sci. Total Environ. 906, 167444.
Jay, J.G., Tyler-Plog, M., Brown, S.L., Grothkopp, F., 2019. Nutrient, metal, and organics removal from stormwater using a range of bioretention soil mixtures. J. Environ. Qual. 48 (2), 493–501.
Kissa, E., 2001. Fluorinated Surfactants and Repellents, 97. CRC Press.
LaFond, J.A., Hatzinger, P.B., Guelfo, J.L., Millerick, K., Jackson, W.A., 2023. Bacterial transformation of per-and poly-fluoroalkyl substances: a review for the field of bioremediation. Environ. Sci. 2 (8), 1019–1041.
LaFond, J.A., Rezes, R., Shojaei, M., Anderson, T., Jackson, W.A., Guelfo, J.L., Hatzinger, P.B., 2024. Biotransformation of PFAA precursors by oxygenase-expressing bacteria in AFFF-impacted groundwater and in pure-compound studies with 6: 2 FTS and EtFOSE. Environ. Sci. Technol. 58 (31), 13820–13832.
Li, K., Gao, P., Xiang, P., Zhang, X., Cui, X., Ma, L.Q., 2017. Molecular mechanisms of PFOA-induced toxicity in animals and humans: implications for health risks. Environ. Int. 99, 43–54.
Liu, C.J., Werner, D., Bellona, C., 2019. Removal of per-and polyfluoroalkyl substances (PFASs) from contaminated groundwater using granular activated carbon: a pilot-scale study with breakthrough modeling. Environ. Sci. 5 (11), 1844–1853.
Lu, Y., Guan, R., Zhu, N., Hao, J., Peng, H., He, A., Zhao, C., Wang, Y., Jiang, G., 2024. A critical review on the bioaccumulation, transportation, and elimination of per-and

polyfluoroalkyl substances in human beings. Crit. Rev. Environ. Sci. Technol. 54 (2), 95–116.
McCleaf, P., Englund, S., Östlund, A., Lindegren, K., Wiberg, K., Ahrens, L., 2017. Removal efficiency of multiple poly-and perfluoroalkyl substances (PFASs) in drinking water using granular activated carbon (GAC) and anion exchange (AE) column tests. Water Res. 120, 77–87.
Mesonet, W.T., 2025. Daily Precipitation Data. Texas Tech University. https://www.mesonet.ttu.edu/.
Milinovic, J., Lacorte, S., Vidal, M., Rigol, A., 2015. Sorption behaviour of perfluoroalkyl substances in soils. Sci. Total Environ. 511, 63–71.
Olmsted, J.L., Ahmadireskety, A., Da Silva, B.F., Robey, N., Aristizabal-Henao, J.J., Bonzongo, J.-C.J., Bowden, J.A., 2021. Using regulatory classifications to assess the impact of different land use types on per-and polyfluoroalkyl substance concentrations in stormwater pond sediments. J. Environ. Eng. 147 (10), 06021005.
Prevedouros, K., Cousins, I.T., Buck, R.C., Korzeniowski, S.H., 2006. Sources, fate and transport of perfluorocarboxylates. Environ. Sci. Technol. 40 (1), 32–44.
Pritchard, J.C., Hawkins, K.M., Cho, Y.-M., Spahr, S., Struck, S.D., Higgins, C.P., Luthy, R. G., 2022. Black Carbon-Amended Engineered Media Filters For Improved Treatment of Stormwater Runoff, 3. ACS Environmental Au, pp. 34–46.
Sarti, C., Souleymane, A.A., Dotro, G., Cincinelli, A., Lyu, T., 2025. Partitioning and removal of per-and polyfluoroalkyl substances (PFAS) in full-scale surface flow treatment wetlands with different upstream wastewater treatment. J. Water Process Eng. 71, 107236.
Schaefer, C.E., Hooper, J.L., Strom, L.E., Abusallout, I., Dickenson, E.R., Thompson, K.A., Mohan, G.R., Drennan, D., Wu, K., Guelfo, J.L., 2023. Occurrence of quantifiable and semi-quantifiable poly-and perfluoroalkyl substances in united states wastewater treatment plants. Water Res. 233, 119724.
Scholz, M., 2015. Wetland Systems to Control Urban Runoff. Elsevier.
Scholz, M., Yang, Q., 2010. Guidance on variables characterising water bodies including sustainable flood retention basins. Landsc. Urban Plan. 98 (3–4), 190–199.
Shi, W., Zhang, Z., Li, M., Dong, H., Li, J., 2024. Reproductive toxicity of PFOA, PFOS and their substitutes: a review based on epidemiological and toxicological evidence. Environ. Res. 250, 118485.
Shojaei, M., Kumar, N., Chaobol, S., Wu, K., Crimi, M., Guelfo, J., 2021. Enhanced recovery of per-and polyfluoroalkyl substances (PFASs) from impacted soils using heat activated persulfate. Environ. Sci. Technol. 55 (14), 9805–9816.
Simonich, S.M., Field, J., Babbar-Sebens, M., Radniecki, T., & Wilson, G. (2022). *Development, evaluation, and technology transfer of BMPs for optimizing removal of PAHs, PCBs, PFAS, and metals from stormwater at DoD sites.* https://sepub-demo-0001-124733793621-us-gov-west-1.s3.us-gov-west-1.amazonaws.com/s3fs-public/2024-01/ER18-1230%20Final%20Report.pdf?VersionId=xAPl42VkOYN0IRSO7C6Z7VP5Zx2p8Ged.
Suja, F., Pramanik, B.K., Zain, S.M., 2009. Contamination, bioaccumulation and toxic effects of perfluorinated chemicals (PFCs) in the water environment: a review paper. Water Sci. Technol. 60 (6), 1533–1544.
Tsuda, S., 2016. Differential toxicity between perfluorooctane sulfonate (PFOS) and perfluorooctanoic acid (PFOA). J. Toxicol. Sci. 41 (Special), SP27–SP36.
USEPA. (1997). "Method 300.1: determination of inorganic anions in drinking water by ion chromatography," Revision 1.0. Cincinnati, OH.
Zareitalabad, P., Siemens, J., Hamer, M., Amelung, W., 2013. Perfluorooctanoic acid (PFOA) and perfluorooctanesulfonic acid (PFOS) in surface waters, sediments, soils and wastewater–a review on concentrations and distribution coefficients. Chemosphere 91 (6), 725–732.